Pergamon

Acta mater. 49 (2001) 3039–3049

Acta MATERIALIA

www.elsevier.com/locate/actamat

METAL FILM CRAWLING IN INTERCONNECT STRUCTURES CAUSED BY CYCLIC TEMPERATURES

M. HUANG[1], Z. SUO[1]† and Q. MA[2]

[1]Department of Mechanical and Aerospace Engineering and Princeton Materials Institute, Princeton University, Princeton, NJ 08544, USA and [2]Intel Corporation, 2200 Mission College Blvd, Santa Clara, CA 95052, USA

(Received 7 March 2001; received in revised form 7 May 2001; accepted 7 May 2001)

Abstract—Thermal cycling is widely used as a qualification test in the microelectronic industry. This paper investigates an intriguing failure mode observed in such a test. Near the corners of a silicon die, shear stresses arise due to thermal expansion mismatch between the silicon and the packaging substrate. These shear stresses may have a small magnitude, being transmitted through packaging polymers, but sometimes motivate metallic interconnect films to crawl toward the center of the die during thermal cycling, even when the temperatures are low and the metal creeps negligibly. The phenomenon has been observed for two decades, but no mechanistic explanation has been given so far. This paper shows that the metal films can crawl by ratcheting plastic deformation. When the temperature cycles, the thermal expansion mismatch between the silicon and the metal causes the metal films to yield. Directed by the small shear stresses, the films shear plastically by a small amount in each cycle, and accumulate a large deformation after many cycles. We develop an idealized model to demonstrate this mechanism, and to study the effects of temperature-dependent yield strength and strain hardening. Several analytical solutions are obtained. Implications for the qualification test and interconnect design are discussed. The study clearly shows the need for basic research on large plastic deformation at small length scales.

Keywords: Thermal cycling

1. INTRODUCTION

Thermal cycling is widely used in the microelectronic industry as a test to qualify new products. The test cycles a device between two temperatures hundreds and thousands of times. Failure modes include die–substrate debonding [1, 2], solder bump detachment [3], die cracking [4, 5], passivation film cracking [6–11], and excessive deformation of metal films [7, 12, 13]. Understanding these failure modes is urgently needed in order to interpret the qualification test and guide new designs. This paper focuses on a particular failure mode: the excessive deformation of metal films, which we will call *crawling* for reasons that will become clear later.

Figure 1 illustrates a part of an interconnect structure before and after about 1000 cycles between −55°C and 125°C. The aluminum films deformed substantially, and even broke the SiN passivation layer. The displacement of the aluminum films was toward the die center, and was maximum near the die corners and gradually reduced on moving away from the corners. Figure 2(a) sketches a flip-chip assembly, of which the interconnect structure in Fig. 1 was a small part. Because of the mismatch of thermal expansion between the packaging substrate and the silicon die, upon cooling from the curing temperature,

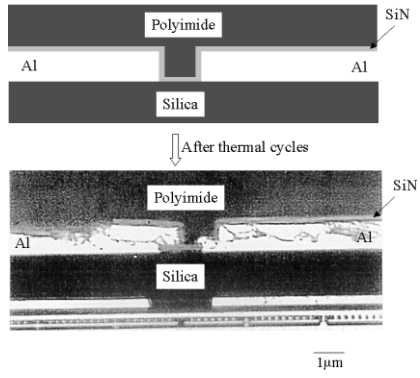

Fig. 1. A schematic of a part of an interconnect structure before thermal cycling, and a micrograph of the same structure after thermal cycling.

† To whom all correspondence should be addressed. Tel.: +1-609-258-0250; fax: +1-609-258-6123.
E-mail address: suo@princeton.edu (Z. Suo)

1359-6454/01/$20.00
PII: S1359-6454(01)00196-3

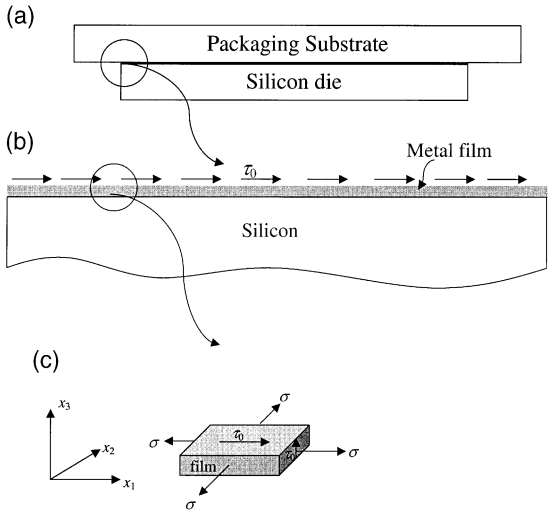

Fig. 2. (a) Schematic of a flip-chip assembly. (b) A magnified view of the left corner of the silicon die, showing the shear stress on the metal film. (c) The stress state in the film.

shear stresses developed at the corners of the die surface [7, 8, 14] [Fig. 2(b)]. Because the thermal expansion coefficient of the packaging substrate was larger than that of silicon, the shear stresses pointed to the die center, consistent with the metal displacement direction. The stresses were gradually reduced on moving away from the corners, as was the observed displacement of the metal films. The shear stresses, however, were limited by the yield strength of the polymer, which was lower than the yield strength of aluminum. How could such small shear stresses plastically deform the aluminum films? Why did this happen after the *cyclic* temperature change?

Metal film crawling under cyclic temperature has been observed for over two decades [7, 12, 13], but its mechanism has never been explained. In this paper, we use the concept of ratcheting to explain this phenomenon. Under the cyclic temperature change, the thermal expansion mismatch between the metal and the silica or silicon underneath causes the metal films to deform plastically. Directed by the shear stresses, the metal films gain a small amount of plastic deformation in each cycle. After many cycles, the accumulated deformation is very large. Ratcheting plastic deformation has been observed in pressure vessels [15], composites [16], multilayers [11, 17], thermal barrier coatings [18, 19], and other engineering structures [20, 21].

The plan of the paper is as follows. Section 2 develops an idealized model of a blanket film on a semi-infinite substrate subject to a constant shear stress and temperature cycles. In Section 3, the film is taken to be elastic and perfectly plastic. Section 4 compares the prediction of the idealized model with a finite element model of a film of finite length. Sections 5 and 6 consider the effects of temperature-dependent yield strength and strain hardening. Throughout the paper, we will relate the idealized model to the practical concerns of the qualification test on the one hand and the basic description of plasticity on the other.

2. A BLANKET FILM ON A SEMI-INFINITE SUBSTRATE

This section develops an idealized model to demonstrate the main concept of crawling. Figure 2(b) illustrates a blanket metal film bonded onto a semi-infinite elastic substrate. Cycle the system between temperatures T_L and T_H. A shear stress, τ_0, acts on the surface of the film. The length scale of interest is much smaller than the overall package, so that the shear stress is taken to be spatially uniform, limited by the yield strength of the polymer used in the package. The cycling temperature range is below the curing temperature of the polymer, so that the shear stress always points to the same direction (i.e. toward the die center) as the temperature changes. To simplify the discussion, we further assume that τ_0 is independent of the temperature. As will become evident, a temperature-dependent τ_0 would not change the qualitative picture. Detailed calculations (e.g. [14]) have shown that a stress normal to the interface, i.e. the peal stress, also exists at the die corner. To focus on the main ideas, we will ignore the peal stress. The biaxial stress in the film, σ, is uniform in the film, and changes with the temperature.

Under these assumptions, the stress field in the system is very simple. The substrate is subject to the shear stress τ_0, but no other stress components. Let the coordinates in the plane of the film be x_1 and x_2, the coordinate normal to the plane be x_3, and the coordinate x_1 coincide with the direction of the shear stress τ_0. As shown in Fig. 2(c), the film is in a uniform stress state of a combination of a biaxial stress and a shear stress:

$$\sigma_{11} = \sigma_{22} = \sigma,\ \sigma_{13} = \tau_0,\ \sigma_{23} = \sigma_{12} = 0. \qquad (1)$$

Obviously the uniform stress states in the substrate and in the film satisfy the equilibrium conditions.

We next consider deformation compatibility between the film and the substrate. Let α_f and α_s be the thermal expansion coefficients of the film and the substrate, respectively ($\alpha_f > \alpha_s$). The semi-infinite substrate is under no in-plane stress. Consequently, when the temperature changes by dT, the in-plane strain of the substrate changes by $\alpha_s\,\mathrm{d}T$. Because the film is bonded to the substrate, the in-plane strain increment of the film equals that of the substrate, namely,

$$\mathrm{d}\varepsilon^p + \mathrm{d}\varepsilon^e + \alpha_f\,\mathrm{d}T = \alpha_s\,\mathrm{d}T, \qquad (2)$$

where ε^p and ε^e are the plastic and the elastic in-plane strain in the film, respectively. That is, the thermal

expansion mismatch is accommodated by a combination of elastic and plastic strains in the film.

The elastic in-plane strain of the film relates to the biaxial stress in the film by Hooke's law:

$$d\varepsilon^e = \frac{1-\nu}{E} d\sigma, \tag{3}$$

where E is Young's modulus and ν is Poisson's ratio of the film. The elastic shear strain in the film is constant at all temperatures, given by

$$\gamma^e = \frac{2(1+\nu)}{E}\tau_0. \tag{4}$$

When the film is elastic, $d\varepsilon^p = 0$, and a combination of equations (2) and (3) gives the biaxial stress increment

$$d\sigma = -\frac{E}{1-\nu}(\alpha_f - \alpha_s)dT. \tag{5}$$

When the film is elastic, the thermal mismatch is entirely accommodated by the elastic strain in the film.

We adopt the J_2 flow theory to analyze the plastic deformation in the film [22], and comment on its suitability for films of submicrometer thickness as we move along. The mean stress in the film is $\sigma_m = 2\sigma/3$. The deviatoric stress tensor, $s_{ij} = \sigma_{ij} - \sigma_m\delta_{ij}$, has the components

$$\begin{aligned} &s_{11} = s_{22} = \sigma/3,\ s_{33} = -2\sigma/3, \\ &s_{13} = \tau_0,\ s_{23} = s_{12} = 0. \end{aligned} \tag{6}$$

The von Mises equivalent stress is

$$\sigma_e = \sqrt{\sigma^2 + 3\tau_0^2}. \tag{7}$$

The J_2 flow theory dictates that the plastic strain increment tensor be in the same direction as the deviatoric stress tensor, namely,

$$d\varepsilon_{ij}^p = s_{ij}\, d\lambda, \tag{8}$$

where $d\lambda$ is a scalar factor of proportionality. Denote $\gamma^p = 2\varepsilon_{13}^p$ as the plastic shear strain in the film. Substituting equation (6) into equation (8), we obtain that

$$\frac{d\varepsilon^p}{\sigma/3} = \frac{d\gamma^p}{2\tau_0} = d\lambda. \tag{9}$$

This relation is the key to the understanding of metal film crawling. During plastic deformation, $d\varepsilon^p$ has the same sign as the biaxial stress σ, and $d\gamma^p$ has the same sign as the shear stress τ_0. When the temperature increases and the film yields in compression ($\sigma<0$), the plastic in-plane strain decreases, $d\varepsilon^p<0$. When the temperature decreases and the film yields in tension ($\sigma>0$), the plastic in-plane strain increases, $d\varepsilon^p>0$. Because the film is bonded to the substrate, for a given temperature increment, $d\varepsilon^p$ is always finite. Consequently, according to equation (9), in each cycle, γ^p increases by a finite amount in the direction of τ_0 when the film is in both tension *and* compression. It is this feature that causes the film to crawl in the same direction as the temperature cycles.

In the previous paragraph, we have based our explanation of crawling on equation (9), which is a consequence of the J_2 flow theory. It is uncertain to what extent the J_2 flow theory is applicable to metal films of submicrometer thickness. However, the crawling mechanism proposed here is robust, quite independent of the detailed flow rules. The film will crawl if (i) the thermal expansion mismatch causes the film to yield; (ii) during yielding, the film gains a finite plastic shear strain, as well as a finite plastic in-plane strain; and (iii) the plastic shear strain is always in the same direction as the shear stress. Because no secure description of micro-plasticity exists, to carry out explicit calculations we will use the J_2 flow theory throughout this paper. Consequently, the quantitative results should be used with caution, but the qualitative trends should be reliable. Of course, the idealized model can be analyzed again when flow laws more appropriate for thin films become available.

Substituting equation (3) into equation (2) gives the increment of the plastic in-plane strain

$$d\varepsilon^p = -(\alpha_f - \alpha_s)dT - \frac{1-\nu}{E}d\sigma. \tag{10}$$

The plastic strain in the film equals the thermal misfit strain minus the elastic strain. Substituting equation (10) into the J_2 flow rule, equation (9) gives the increment of the plastic shear strain

$$d\gamma^p = -\frac{6\tau_0}{\sigma}\left[(\alpha_f - \alpha_s)dT + \frac{1-\nu}{E}d\sigma\right]. \tag{11}$$

To integrate equations (10) and (11), further specification of the plastic flow is needed to determine $d\sigma$ for a given dT. The following sections discuss three cases in detail: (a) the film is non-hardening and the yield strength is independent of the temperature; (b) the film is non-hardening but the yield strength depends on the temperature; and (c) the film is strain hardening but the yield strength is independent of the temperature.

3. ELASTIC AND PERFECTLY PLASTIC FILM

This section assumes that the uniaxial yield strength of the metal, Y, is constant, independent of the temperature and the amount of the plastic strain. The von Mises yield condition is specialized to

$$\sigma^2 + 3\tau_0^2 = Y^2. \tag{12}$$

When the film yields, the biaxial stress can only be at one of the two levels:

$$\sigma = \pm\sqrt{Y^2 - 3\tau_0^2}. \tag{13}$$

The biaxial stress remains fixed, $d\sigma = 0$, as the film deforms plastically. Equations (10) and (11) give the increment of the plastic in-plane strain

$$d\varepsilon^p = -(\alpha_f - \alpha_s)dT, \tag{14}$$

and the increment of the plastic shear strain

$$d\gamma^p = -\frac{6\tau_0(\alpha_f - \alpha_s)}{\sigma}dT. \tag{15}$$

When the film plastically deforms in tension, $\sigma = +\sqrt{Y^2 - 3\tau_0^2}$ and $dT<0$. When the film plastically deforms in compression, $\sigma = -\sqrt{Y^2 - 3\tau_0^2}$ and $dT>0$. In both cases, the plastic shear strain increment is in the same direction of τ_0, namely, $d\gamma^p>0$, giving rise to crawling.

Figure 3(a) shows the prescribed temperature change with time. Figures 3(b–d) show the biaxial stress, the plastic in-plane strain, and the plastic shear strain as functions of the temperature. These figures are described in detail as follows. They help to develop an intuition for crawling.

State A. $T = T_L$. The initial biaxial stress in the film is taken to be σ_i, the exact value of which only affects the first cycle, so long as the film remains elastic under the combined initial biaxial stress and the shear stress, namely, $\sigma_i^2 + 3\tau_0^2 < Y^2$.

Path AB. $T_L<T<T_B$. The rising temperature causes thermal expansion in the film, but the film is elastic. The biaxial stress changes toward compression, as described by equation (3), and represented in Fig. 3(b) by a straight line with the slope $-E(\alpha_f - \alpha_s)/(1-\nu)$. The film gains no plastic strains, as shown in Figs 3(c) and 3(d) by the horizontal lines.

State B. $T = T_B$. The film yields in compression, reaching the biaxial stress $\sigma = -\sqrt{Y^2 - 3\tau_0^2}$.

Path BC. $T_B<T<T_H$. The film deforms plastically in compression. The biaxial stress keeps at the constant level, as represented by the horizontal line in Fig. 3(b). When the temperature increases, the plastic in-plane strain decreases according to equation (14), represented in Fig. 3(c) by a straight line of the slope $-(\alpha_f - \alpha_s)$. Meanwhile, the plastic shear strain increases according to equation (15), represented in Fig. 3(d) by a straight line of slope $6\tau_0(\alpha_f - \alpha_s)/\sqrt{Y^2 - 3\tau_0^2}$.

State C. $T = T_H$. The system reaches the prescribed highest temperature.

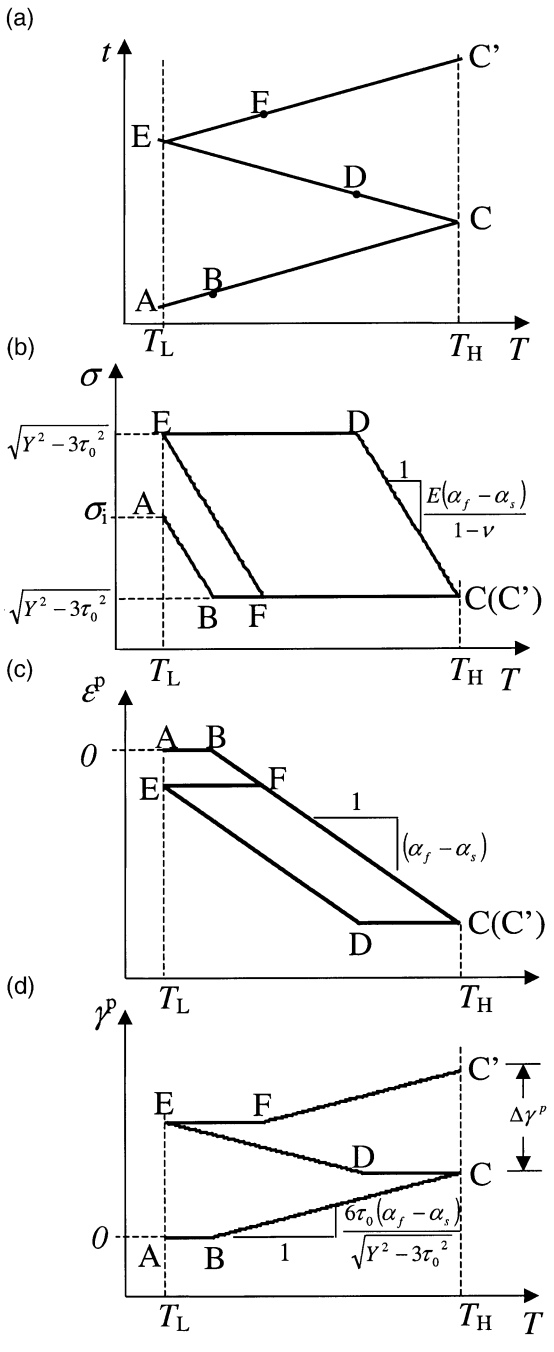

Fig. 3. Predictions of the model of an elastic and perfectly plastic film with a temperature-independent yield strength: (a) the prescribed temperature changes with time; (b) the biaxial stress as a function of the temperature; (c) the plastic in-plane strain as a function of the temperature; (d) the plastic shear strain as a function of the temperature.

Path CD. $T_H > T > T_D$. The dropping temperature causes thermal contraction in the film. The biaxial stress changes toward tension. The film is elastic and gains no plastic strain.

State D. $T = T_D$. The metal film yields in tension, reaching the biaxial stress $\sigma = +\sqrt{Y^2 - 3\tau_0^2}$.

Path DE. $T_D > T > T_L$. The biaxial stress remains at the constant level, as represented by the horizontal line in Fig. 3(b). The dropping temperature causes thermal contraction in the film. The film deforms plastically in tension. The plastic in-plane strain increases according to equation (14), and the plastic shear strain increases according to equation (15).

State E. $T = T_L$. The system reaches the prescribed lowest temperature.

Path EF. $T_L < T < T_F$. The rising temperature causes thermal expansion in the film. The film deforms elastically, changing the biaxial stress toward compression.

State F. $T = T_F$. The film yields again in compression, reaching the biaxial stress $\sigma = -\sqrt{Y^2 - 3\tau_0^2}$.

Path FC′. $T_F < T < T_H$. The biaxial stress remains constant. The film deforms plastically according to equations (14) and (15).

State C′. $T = T_H$. The temperature reaches the prescribed highest point.

Starting from state C′, as the temperature cycles, the biaxial stress and the in-plane strain cycle around the loop CDEF. The shear strain, however, *increases* by a definite amount each cycle.

Figure 4 shows a coordinate plane spanned by the normalized shear stress, τ_0/Y, and the normalized temperature range, $E(\alpha_f - \alpha_s)(T_H - T_L)/(1-\nu)Y$. The plane is divided into three regimes: plastic collapse, shakedown, and crawling (or ratcheting). Figures of this type are known as Bree diagrams [15]. If $(\tau_0/Y) \geq (1/\sqrt{3})$, the film plastically deforms under the shear stress alone without the aid of the temperature change, and the device is in the plastic collapse regime. If $(\tau_0/Y) < (1/\sqrt{3})$ and the temperature range is small enough, the device may plastically deform during the first temperature cycle, but cycles elastically afterward. The device is in the shakedown regime. From Fig. 3(b), we see that the film shakes down if states D and E coincide, namely,

$$2\sqrt{Y^2 - 3\tau_0^2} \geq \frac{E(\alpha_f - \alpha_s)(T_H - T_L)}{(1-\nu)}. \tag{16}$$

This shakedown condition is represented in Fig. 4 by a shaded region below a quarter of an elliptical curve. Outside the shaded region, if $\tau_0 = 0$, the temperature change causes cyclic in-plane strain but no shear strain. If $\tau_0 > 0$ and the temperature change is large enough, the film will crawl. In the crawling regime, the in-plane strain cycles plastically, but the shear strain increases by a fixed amount each cycle. The crawling rate (i.e. the plastic shear strain increment per cycle) is represented by CC′ in Fig. 3(d), given by

$$\Delta\gamma^p = \frac{12(1-\nu)\tau_0}{E}\left[\frac{E(\alpha_f - \alpha_s)(T_H - T_L)}{(1-\nu)\sqrt{Y^2 - 3\tau_0^2}} - 2\right]. \tag{17}$$

Contours of constant crawling rate are mapped in the crawling regime. Thomas [13] used the amount of crawling after a given number of cycles as an experimental method to screen various polymers developed for "low stress" applications. Equation (17) provides a theoretical basis for this method, provided τ_0 is interpreted as the stress transmitted through the polymers.

The practical implications of the Bree diagram (Fig. 4) are as follows. A given pair of the normalized shear stress and the normalized temperature range corresponds to a point in the diagram. If the point falls in the plastic collapse regime, the design must be modified either to decrease the yield strength of the polymer, or to increase the yield strength of the metal film, in order to bring the structure out of the plastic collapse regime. If the point falls in the shakedown regime, the film may deform plastically for the first temperature cycle and will remain elastic afterwards. The shakedown regime should be the design goal. If the point falls in the crawling regime, the film will shear incrementally as the temperature cycles. For example, if a point falls on the curve labeled $E\,\Delta\gamma^p/[(1-\nu)Y] = 1$, using the material properties in Table 1, we predict that the film crawls $\Delta\gamma^p \cong 10^{-3}$ per cycle, so that a film of thickness 1 μm crawls by a distance of 1 μm after 1000 cycles. Using the material properties in Table 1, we find that the maximum temperature range for the film to be in the shakedown regime is about 100°C. When the device is cycled beyond this temperature range, the film will crawl, no

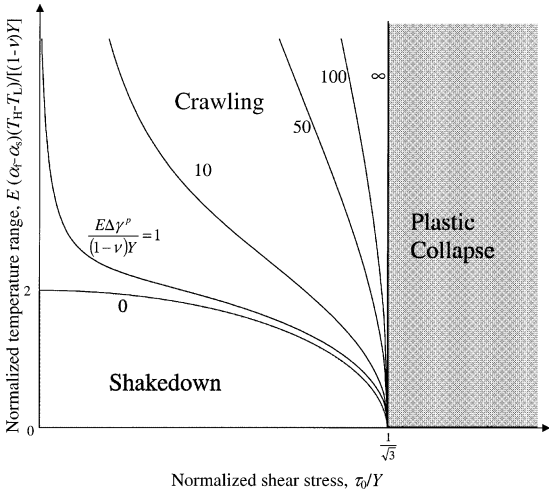

Fig. 4. The Bree diagram for the elastic and perfectly plastic film. The plane spanned by the normalized shear stress and temperature range is divided into three regimes: plastic collapse, shakedown, and crawling. The contours of plastic shear strain per cycle are mapped in the ratcheting regime.

Table 1. Material properties used in finite element calculations

E_{film} (GPa)	E_{sub} (GPa)	ν_{film}	ν_{sub}	Y (MPa)	$(\alpha_f-\alpha_s)$ (1/°C)
70	200	0.33	0.2	100	20×10^{-6}

matter how small the shear stress is, so long as the shear stress does not vanish. The shakedown temperature range can be extended if the yield strength of the metal film is larger, or if the thermal expansion mismatch, $E(\alpha_f-\alpha_s)$, is smaller. To accelerate the qualification test, the engineer sometimes uses a temperature range larger than that intended in the normal use of the device. If crawling is observed in the qualification test, the engineer should not conclude that the device is unsafe in use. A simple-minded extrapolation can also be misleading, for a smaller temperature range may bring the device into the shakedown regime.

4. A FINITE ELEMENT MODEL OF A FILM OF FINITE LENGTH

The object of this section is to show that the model for blanket films also predicts the crawling rate of films of finite lengths. In the blanket film the stresses are spatially uniform. In a film of finite length, however, the stresses are non-uniform as the film edges are approached. The problem of films of finite lengths cannot be solved analytically. Instead we use the commercial finite element software ABAQUS, adopting three-node triangular plane strain elements. The thickness of the films are $h = 1$ μm. Films of two lengths, $L = 10$ μm and $L = 100$ μm, are studied. The shear stress applied to the surface of the films is $\tau_0 = 50$ MPa. The temperature cycles between 0°C and 140°C. To ensure that the deformation is in the plane strain state as the temperature changes, we set the thermal expansion coefficient of the substrate to be zero, and the thermal expansion coefficient of the films to be $(\alpha_f-\alpha_s)$. Table 1 shows the material properties used in the finite element calculations. Of the numerical values used in the finite element calculation, τ_0 and Y are uncertain, that is they may not correspond to those in the experimental observation (Fig. 1). The purpose of this calculation is to ascertain the validity of the blanket film model.

Define the average shear strain at a point along the film as the displacement of the film surface relative to the substrate surface, Δu, divided by the thickness of the film, h. Figure 5 shows the average shear strain, $\Delta u/h$, along the film at several temperatures. In state A, the film is only under the shear stress, the biaxial stress is set to be zero, and the shear strains at the front edge and the back edge are symmetrically distributed. The film deforms plastically at the two edges to particularly relieve the stress concentration. When the temperature increases to state B, thermal expansion increases the average shear strain at the front edge, but decreases the average shear strain at the back edge. Meanwhile the middle part of the film remains elastic and does not shear further relative to state A. When the temperature increases to state C, the entire film has yielded. The middle part of the film deforms plastically to the right, the front edge moves to the right, and the back edge moves to the left. The system reaches the highest temperature in state D. The shear strain increases a lot at the front edge and in the middle of the film, but only changes a little at the back edge. In state E, the shear strain of the back edge increases. In state G, the lowest temperature, the shear strain increases a lot at the back edge, but only changes a little at the front edge. After one thermal cycle, the whole film shears toward the right. The film crawls as if the two edges were two legs, taking turns to move.

Figure 6 shows the accumulated average shear strain of the middle part of the film as a function of the number of cycles. The solid line is the prediction of the theory for the blanket film, and the data points are the results of the finite element calculation for the 100 μm and 10 μm films. The shear strain at the middle part of the film is insensitive to the film length. The idealized model predicts well the crawling rate even for very short films.

The state in a finite film is well approximated by that in a blanket film, except for short lengths at the two edges. These short lengths can be estimated by the shear lag model (e.g. [23]). As shown in Fig. 5, at the back edge the stress component σ_{11} vanishes at the ends of the film, and builds up to the level $\sqrt{Y^2-3\tau_0^2}$ over the length L_s. For the film to slide plastically, the shear stress at the film/substrate interface should be the shear yield strength, $Y/\sqrt{3}$. Force balance requires that

$$L_s = \sqrt{3}h\sqrt{\frac{Y+\sqrt{3}\tau_0}{Y-\sqrt{3}\tau_0}}. \tag{18}$$

The theory of the blanket film predicts well the shear strains in the middle part of the finite film, if the total film length exceeds twice the shear lag length, $L>2L_s$.

5. TEMPERATURE-DEPENDENT YIELD STRENGTH

Numerous wafer curvature measurements have shown that the yield strength of metal films depends on temperature (e.g. [24, 25]). We now study the effect of the temperature-dependent yield strength on crawling. Assume that the yield strength of the metal film is a function of the temperature, $Y = Y(T)$. At a

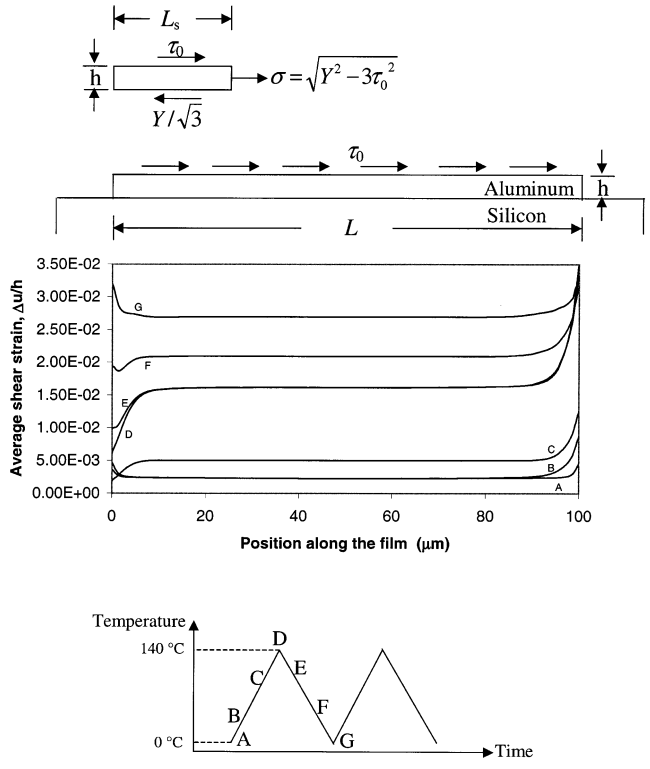

Fig. 5. Model of a film of a finite length. Finite element results are shown for a film of length 100 μm.

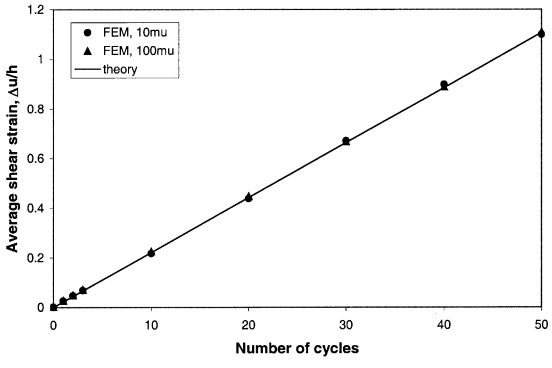

Fig. 6. Accumulated average shear strain of the middle part of the film as a function of the number of cycles.

given temperature, the film is still taken to be an elastic and perfectly plastic solid, satisfying the von Mises yield condition

$$\sigma^2 + 3\tau_0^2 = Y^2. \tag{19}$$

We could also assume τ_0 to be a function of temperature. The treatment would be similar to what follows and will not be pursued in this paper. When the film deforms plastically, for a given temperature increment dT, equation (19) gives the biaxial stress increment in the film

$$\mathrm{d}\sigma = \frac{Y}{\sigma}\frac{\mathrm{d}Y}{\mathrm{d}T}\mathrm{d}T. \tag{20}$$

Substituting equation (20) into equations (10) and (11), we obtain the plastic in-plane strain increment

$$\mathrm{d}\varepsilon^p = -\left[(\alpha_f - \alpha_s) + \frac{(1-\nu)Y}{E\sigma}\frac{\mathrm{d}Y}{\mathrm{d}T}\right]\mathrm{d}T, \tag{21}$$

and the plastic shear strain increment

$$\mathrm{d}\gamma^p = -\frac{6\tau_0}{\sigma}\left[(\alpha_f - \alpha_s) + \frac{(1-\nu)Y}{E\sigma}\frac{\mathrm{d}Y}{\mathrm{d}T}\right]\mathrm{d}T, \tag{22}$$

For a complete temperature cycle, the net temperature change is zero, and so are the net changes in the yield strength and the biaxial stress. Integrating equation (21) for a complete cycle, we can show that the net change in the plastic in-plane strain is zero.

To illustrate the effect of the temperature-dependent yield strength, we assume that the yield strength is a linear function of the temperature:

$$Y = Y^0 - \beta(T - T^0), \tag{23}$$

where Y^0, β, and T^0 are all constants. Figure 7 sketches the biaxial stress, plastic in-plane strain, and plastic shear strain as functions of the temperature. They are qualitatively the same as those for a film

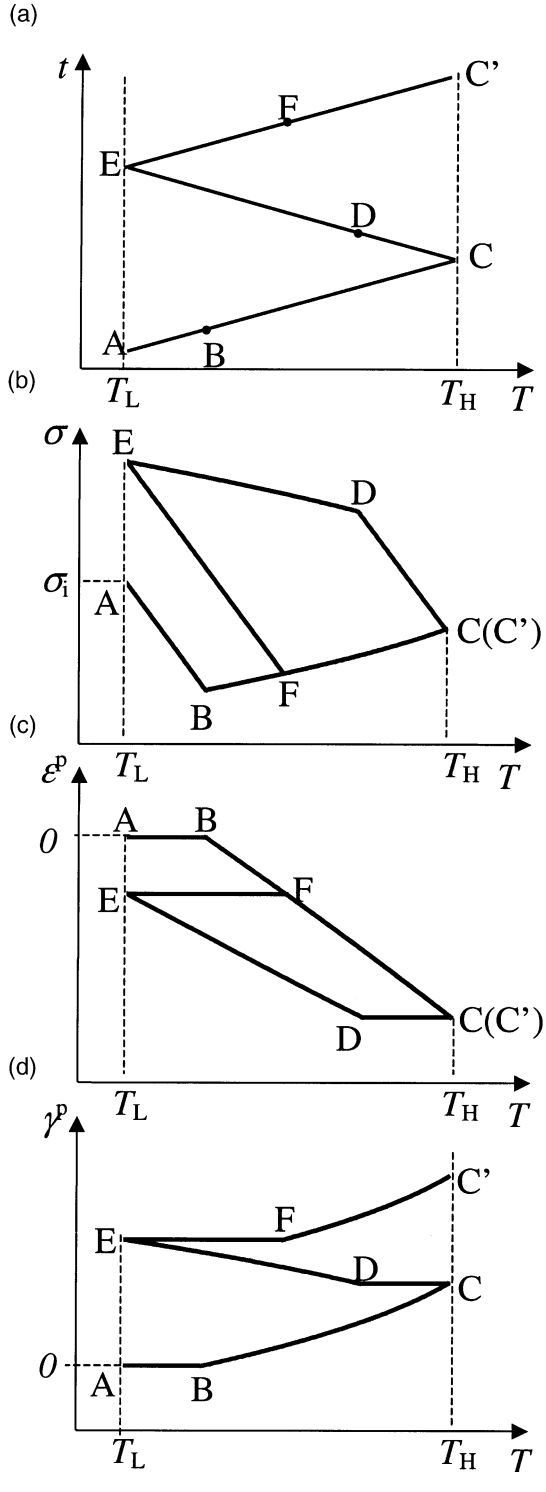

Fig. 7. Elastic and perfectly plastic film with temperature-dependent yield strengths: (a) the prescribed temperature changes with time; (b) the biaxial stress as a function of the temperature; (c) the plastic in-plane strain as a function of the temperature; (d) the plastic shear strain as a function of the temperature.

with a temperature-independent yield strength (Fig. 3).

6. STRAIN HARDENING FILM

Because the film crawls by accumulating a large amount of plastic deformation, strain hardening plays an important role, so long as the temperatures are low enough that the film does not anneal [26]. In the elastic state, the film behaves the same as discussed before. This section focuses on the effect of isotropic hardening on the plastic state. Prior to thermal cycling, the fabrication process (the temperature changes, materials integration steps, etc.) will cause plastic deformation in the metal film. As a result, the yield strength of the film after the fabrication process and before the thermal cycles, Y_0, is usually higher than the initial yield strength measured in a uniaxial tensile test. When the temperature range $(T_H - T_L)$ is below a critical value, the film will be elastic and gains no plastic strain during thermal cycling. The biaxial stress cycles between $\pm E(\alpha_f - \alpha_s)(T_H - T_L)/(1-\nu)$. Consequently, the film will cycle elastically if the effective stress is below Y_0, namely

$$\sqrt{\left[\frac{E(\alpha_f-\alpha_s)(T_H-T_L)}{2(1-\nu)}\right]^2 + 3\tau_0^2} < Y_0. \qquad (24)$$

Figure 8 shows a coordinate plane spanned by the normalized shear stress and the normalized temperature range, where the inequality (24) is represented by the shaded region. When the temperature range is above this region, the thermal cycles cause plastic strains in addition to those caused by the fabrication process. Consequently, for the strain hardening material, the yield strength increases with the thermal

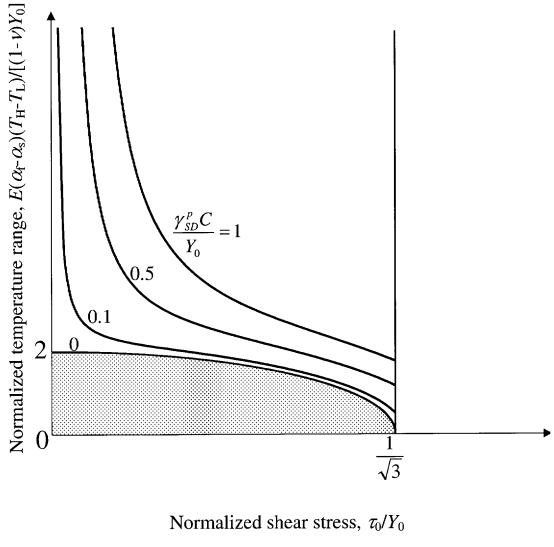

Fig. 8. The plastic shear strain accumulated during the thermal cycles to shake down the film.

cycles. The film asymptotes to a shakedown state, in which the biaxial stress cycles elastically between $\pm E(\alpha_f-\alpha_s)(T_H-T_L)/(1-\nu)$. In the shakedown state, the yield strength of the film becomes constant, given by

$$Y_{SD}=\sqrt{\left[\frac{E(\alpha_f-\alpha_s)(T_H-T_L)}{2(1-\nu)}\right]^2+3\tau_0^2}. \qquad (25)$$

To approach the shakedown state, the cycles increase the yield strength from Y_0 to Y_{SD}.

The above considerations are independent of the detailed hardening law. However, to calculate the amount of plastic strain and the number of cycles to approach the shakedown state, we need to prescribe a hardening law. The following analysis assumes that, in the uniaxial stress state, the yield strength increases linearly with the uniaxial plastic strain, with the proportionality coefficient C. Denote the current yield strength by Y. The J_2 flow theory requires that λ defined in equation (8) be a function of the current yield strength. Fitting this function to the uniaxial stress–strain relation, we obtain that

$$d\lambda=\frac{3}{2CY}dY. \qquad (26)$$

Substituting equation (26) into equation (9), we obtain the plastic in-plane strain increment

$$d\varepsilon^p=\frac{\sigma}{2CY}dY, \qquad (27)$$

and the plastic shear strain increment

$$d\gamma^p=\frac{3\tau_0}{CY}dY. \qquad (28)$$

When the film deforms plastically, $dY>0$. The plastic in-plane strain increases when the film is in tension, and decreases when the film is in compression. The plastic shear strain increases when the film is in both tension and compression.

Integrate equation (28) from the state when the thermal cycles start, Y_0, to the shakedown state, Y_{SD}. The plastic shear strain accumulated over the thermal cycles to shake down the film is

$$\gamma^p_{SD}=\frac{3\tau_0}{C}\ln\left(\frac{Y_{SD}}{Y_0}\right). \qquad (29)$$

The larger the hardening rate C, the less the film needs to crawl to shakedown. Figure 8 plots equation (29). Because $\tau_0<Y_0/\sqrt{3}$, we need only consider the region to the left of the vertical line. As mentioned before, when the shear stress and the temperature range fall into the shaded region, the film is elastic and gains no plastic strain during the thermal cycles. This region is noted in Fig. 8 as $\gamma^p_{SD}C/Y_0=0$. Above the shaded region, γ^p_{SD} increases as the shear stress and the temperature range increases. For example, assuming $C/Y_0=10$ and allowing $\gamma^p_{SD}=0.1$, one can enlarge the design space to the area below the contour $\gamma^p_{SD}C/Y_0=1$. To know the total plastic strain prior to shakedown, one needs to know the plastic strain before thermal cycling, which depends on the fabrication process. This is a very complicated problem by itself, which is beyond the scope of this paper.

Because τ_0 is taken to be constant, the increment of the yield strength, $Y=\sqrt{\sigma^2+3\tau_0^2}$, relates to the increment of the biaxial stress, σ, as $dY=(\sigma/Y)d\sigma$. Substituting equation (27) into equation (10), we relate the increment of the yield strength to the increment of the temperature:

$$\left[\frac{\sigma}{2CY}+\frac{(1-\nu)Y}{E\sigma}\right]dY=-(\alpha_f-\alpha_s)dT. \qquad (30)$$

The equation is valid when the film deforms plastically, where the biaxial stress is given by $|\sigma|=\sqrt{Y^2-3\tau_0^2}$. When $|\sigma|<\sqrt{Y^2-3\tau_0^2}$, the film is elastic and $dY=0$.

After the Nth cycle, the yield strength of the film is Y_N at T_L, and $Y_{N+0.5}$ at T_H. When the temperature increases from T_L to T_H, as seen in Fig. 9(a), the film yields when the temperature reaches

$$T_F=T_L+\frac{2(1-\nu)\sqrt{Y_N^2-3\tau_0^2}}{E(\alpha_f-\alpha_s)}.$$

Integrating equation (30) from T_F to T_H, we obtain that

$$\left[\left(\frac{1}{2C}+\frac{1-\nu}{E}\right)\sqrt{Y^2-3\tau_0^2}-\frac{\sqrt{3}\tau_0}{2C}\tan^{-1}\frac{\sqrt{Y^2-3\tau_0^2}}{\sqrt{3}\tau_0}\right]_{Y_N}^{Y_{N+0.5}}$$
$$=\frac{(1-\nu)\sqrt{Y_N^2-3\tau_0^2}}{E}\left[\frac{E(\alpha_f-\alpha_s)(T_H-T_L)}{(1-\nu)\sqrt{Y_N^2-3\tau_0^2}}-2\right]. \qquad (31)$$

This relation updates the yield strength as a function of N.

Figure 9 shows the yield strength, the biaxial stress, the plastic in-plane strain and the plastic shear strain as functions of temperature from the Nth cycle to the $(N+1)$th cycle. Because the yield strength of the film increases in each cycle, the net change in the biaxial stress and plastic in-plane strain are not zero for a complete temperature cycle, and the plastic shear strain per cycle (i.e. the crawling rate) decreases.

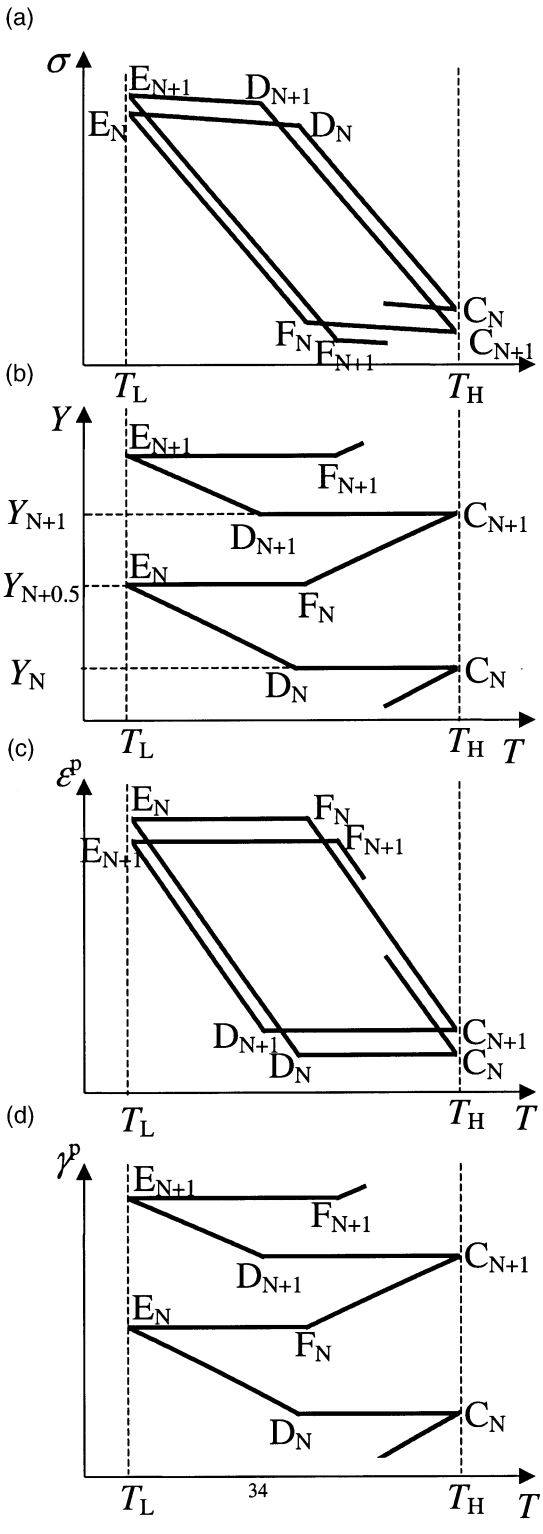

Fig. 9. Strain hardening film with a temperature-independent yield strength: (a) the biaxial stress as a function of the temperature; (b) the yield strength as a function of the temperature; (c) the plastic in-plane strain as a function of the temperature; (d) the plastic shear strain as a function of the temperature.

Figure 10 plots $\ln[(Y_{SD}-Y_0)/(Y_{SD}-Y_N)]$ as a function of the number of cycles, N, by using the material properties in Table 1 and $C/Y_0 = 10$. The function is very close to a straight line, suggesting that the yield strength should increase with the number of cycles according to

$$Y_N \approx Y_{SD} - (Y_{SD}-Y_0)\exp\left(-\frac{N}{N_{SD}}\right). \tag{32}$$

We estimate the characteristic number of cycles to reach shakedown from

$$N_{SD} = \tfrac{1}{2}\lim_{N\to+\infty}\frac{(Y_{SD}-Y_N)}{(Y_{N+0.5}-Y_N)}. \tag{33}$$

By using equations (25) and (31), we obtain that

$$N_{SD} = \frac{1}{4} + \frac{E}{8(1-\nu)C}\frac{1}{1+12\left[\dfrac{(1-\nu)\tau_0}{E(\alpha_f-\alpha_s)(T_H-T_L)}\right]^2}. \tag{34}$$

The value of E/C plays an important role in setting the number of cycles to reach shakedown. Taking the material properties in Table 1 and $C/Y_0 = 10$, we estimate that $N_{SD}\approx 10$. In this case, the film shakes down rapidly.

7. CONCLUDING REMARKS

This paper identifies ratcheting plastic deformation as a mechanism responsible for a failure mode in a qualification test widely used in the microelectronic industry. We analyze an idealized model of a blanket metal film on a semi-infinite substrate, subjected to a constant shear stress and cyclic temperatures. We show that the film can crawl by ratcheting plastic deformation. The phenomenon is expected in model systems such as a thin-walled tube under combined

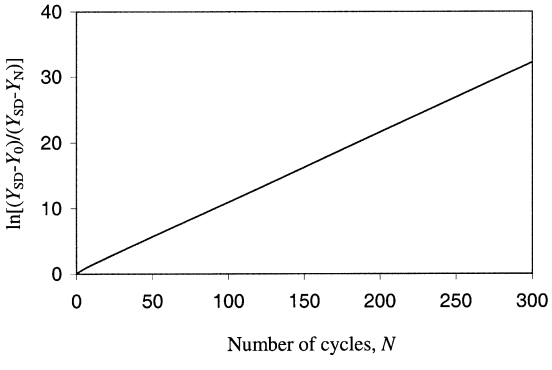

Fig. 10. $\ln[(Y_{SD}-Y_0)]/[(Y_{SD}-Y_N)]$ as a function of the number of temperature cycles.

torsion and axial force, where one stress component cycles and the other stress component points in a fixed direction. The Bree diagram is constructed to aid design and the interpretation of the qualification test. By adjusting the yield strength of the packaging polymer, the yield strength and the strain-hardening rate of the film, and the thermal expansion mismatch between the film and the substrate, one can ensure that the film shakes down after a small amount of crawling. At present, a quantitative comparison between the theory and experiments is impossible. The lack of a secure description of micro-plasticity has forced us to base the calculations on idealized, macroscopic flow rules. Although we argue that different flow rules should not alter the qualitative picture, they will certainly modify the quantitative predictions. Furthermore, wafer curvature experiments are commonly limited to small strain and a few temperature cycles, which would require excessive extrapolations for the present phenomenon. The magnitude of the shear stress τ_0 relates to the nonlinear deformation characteristics of the packaging polymers, which are not well studied. Once more we stress that large plastic deformation for both metals and polymers at small length scales, under multiaxial loads and variable temperatures, has not been adequately studied. Deformation phenomena in microelectronics, such as metal film crawling, provide a strong motivation for experimental and theoretical developments in this fascinating field of plasticity at small length scales.

Acknowledgements—The work at Princeton University has been supported by DARPA and Intel Corporation.

REFERENCES

1. Yan, X. and Agarwal, R. K., *ASME Trans., J. Electron. Packag.*, 1998, **120**, 150.
2. Gurmurthy, C. K., Jiao, J., Norris, L. G., Hui, C. -Y. and Kramer, E. J., *ASME Trans., J. Electron. Packag.*, 1998, **120**, 372.
3. Lau, J., Wong, C. P., Prince, J. L. and Nakayama, W., *Electronic Packaging, Design, Materials, Process, and Reliability*. McGraw Hill, New York, 1998.
4. Han, J. -B., *ASME Trans., J. Electron. Packag.*, 2001, **123**, 58.
5. Michaelides, S. and Sitaraman, S. K., *IEEE Trans. Adv. Packag.*, 1999, **22**, 602.
6. Edwards, D. R., Heinen, K. G., Groothuis, S. K. and Martinez, J. E., *IEEE Trans. Components, Hybrids, Manuf. Technol.*, 1987, **12**, 618.
7. Alpern, P., Wicher, V. and Tilgner, R., *IEEE Trans. Components, Packag., Manuf. Technol.—Part A*, 1994, **17**, 583, Correction in 1995, **18**, 862.
8. Nguyen, L. T., Gee, S. A., Johnson, M. R., Grimm, H. E., Berardi, H. and Walberg, R. L., *IEEE Trans., Components, Packag., Manuf. Technol.—Part A*, 1995, **18**, 15.
9. Pendse, R. D., *IEEE Trans. Components, Hybrids, Manuf. Technol.*, 1991, **14**, 870.
10. Gee, S. A., Johnson, M. R. and Chen, K. L., *IEEE Trans. Components, Packag., Manuf. Technol.—Part B*, 1995, **18**, 478.
11. Huang, M., Suo, Z., Ma, Q. and Fujimoto, H., *J. Mater. Res.*, 2000, **15**, 1239.
12. Isagawa, M., Iwasaki, Y. and Sutoh, T., in *Proc. Int. Reliability Physics Symp.* 1980, p. 171.
13. Thomas, R. E., *IEEE Trans. Components, Hybrids, Manuf. Technol.*, 1985, **8**, 427.
14. Liu, X. H., Suo, Z. and Ma, Q., *Acta mater.*, 1999, **47**, 67.
15. Bree, J., *J. Strain Anal.*, 1967, **2**, 226.
16. Jansson, S. and Leckie, F. A., *J. Mech. Phys. Solids*, 1992, **40**, 593.
17. Begley, M. R. and Evans, A. G., *ASME Trans., J. Appl. Mech.*, in press.
18. Karlsson, A. M. and Evans, A. G., *Acta mater.*, in press.
19. He, M. Y., Evans, A. G. and Hutchinson, J. W., *Acta mater.*, 2000, **48**, 2593.
20. Suresh, S., *Fatigue of Materials*, 2nd edn. Cambridge University, Cambridge, 1998.
21. Ponter, A. R. S. and Cocks, A. C. F., *ASME Trans., J. Appl. Mech.*, 1984, **51**, 465.
22. Hill, R., *The Mathematical Theory of Plasticity*. Clarendon Press, Oxford, 1950.
23. Hu, M. S. and Evans, A. G., *Acta metall.*, 1989, **37**, 917.
24. Nix, W. D., *Metall. Trans.*, 1989, **A20**, 2217.
25. Baker, S. P., Kretschmann, A. and Arzt, E., *Acta mater.*, submitted.
26. Shen, Y. -L., Suresh, S., He, M. Y., Bagchi, A., Kienzle, O., Rühle, M. and Evans, A. G., *J. Mater. Res.*, 1998, **13**, 1928.